D16

N79-24017

ANALYTICAL STUDY OF THE TIME DEPENDENT SPACECRAFT-PLASMA INTERACTION*

J. W. Cipolla, Jr. and M. B. Silevitch
Northeastern University

SUMMARY

A study of the time dependent interaction of an initially uniform equilibrium plasma with a plane conducting surface has been made in order to achieve a more complete understanding of the dynamics of the charging process and of the approach to the floating potential on the surface. Numerical solutions of the cold ion equations of motion in conjunction with equilibrium electrons and Poisson's equation show the formation of an ion-rich sheath near the surface and the coupling of the non-neutral region to the undisturbed plasma through a quasineutral rarefaction. Analytical treatment of the quasineutral region shows excellent agreement (within 1%) with the numerical results.

INTRODUCTION AND FORMULATION OF EQUATIONS

Observations of anomalous behavior in synchronous orbit satellites and the attribution of these effects to the charging of spacecraft by energetic electrons has led to the need for more complete understanding of the dynamic interaction of solid bodies with plasmas. In this work a mathematical model of this time dependent interaction is presented. Previous analytical work on time dependent plasma boundary value problems has been restricted to time dependent probe theory, in which the sheath development and plasma response to a known variation of probe potential is sought (ref. 1-6), to plasma expansion into vacuum (ref. 7-9), and to ion acceleration in a steep density gradient (ref. 10). It is essential to note, however, that in our work (in contrast to these earlier treatments) both the probe potential and plasma response are unknown and linked through the self-consistent set of equations to be set down in further detail below.

Consider a planar conducting slab of arbitrary thickness initially uncharged and in equilibrium with a collisionless neutral stationary plasma (fig. 1). At time $t = 0$ the slab begins to absorb <u>all</u> charge incident upon it but remains non-emitting. This non-emitting catalytic wall assumption is introduced solely for simplicity; the effects of partial absorption and recombination of electrons and ions respectively and of such emissions as photoemission, secondary emission, etc. can be included as adjustments in the boundary conditions of the problem. This physical situation could describe either a planar laboratory probe, a nonplanar laboratory system in contact with a small

*This work was supported by AFOSR contract F19628-76-C-0246 and grant 78-3731.

Debye length plasma, or planar portions of a satellite in contact with the earth's plasma environment. For many conditions of interest, the electron to ion temperature ratio T_e/T_i is equal to or greater than unity, so that the random thermal electron flux initially dominates the ion flux to the boundary, resulting in the buildup of a negative surface charge on both exposed surfaces while the condition of zero electric field is maintained in the slab interior. Since all subsequent development occurs symmetrically, attention is focused on the half space $x > 0$ with the right face of the slab located in the plane $x = 0$, keeping in mind, however, that within one skin depth of the surface the electric field is uniformly zero. It is clear that the initial acquisition of negative surface charge leaves an ion rich layer immediately adjacent to the slab, in which a negative potential and electric field are established due to the initial charge separation. These self-consistent fields then act to decelerate electrons and accelerate ions until a balance between their fluxes is achieved (at least for singly ionized plasmas), at which point no net current flows to the boundary and the process achieves a steady state.

In our further discussion and analytical development it is convenient to make the following assumptions:

1. Plasma electrons, with thermal energy kT_e, are to be treated as always in a quasistatic equilibrium state relative to the ions. Thus the nondimensional electron number density and flux are given by

$$n_e(\psi) = e^{-\psi}\left(1 - \frac{1}{2}\,\mathrm{erfc}\sqrt{\psi_w-\psi}\right)\left(1 - \frac{1}{2}\,\mathrm{erfc}\sqrt{\psi_w}\right)^{-1} \tag{1a}$$

$$j_e(\psi) = -\left(\frac{m_i}{2\pi m_e}\right)^{1/2} e^{-\psi_w}\left(1 - \frac{1}{2}\,\mathrm{erfc}\sqrt{\psi_w}\right)^{-1} \tag{1b}$$

where the dimensional (with tildes) density, flux, potential, and wall potential, respectively, are defined by

$$\tilde{n}_e = n_e n_o\ , \quad \tilde{j}_e = j_e n_o c\ , \quad -\tilde{\phi} = (kT_e/|e|)\psi\ , \quad -\tilde{\phi}(o,t) = (kT_e/|e|)\psi_w$$

where n_o is the density of the undisturbed plasma and $c = (kT_e/m_i)^{1/2}$ is the ion acoustic speed. The complementary error function reflects the halfrange nature of the electron distribution function due to the absorbing boundary and has been discussed in detail by Hu and Zeiring in reference 11. Equations (1a) and (1b) are reasonable since the charging dynamics are expected to scale as the ion plasma period

$$\omega_{pi}^{-1} = (\varepsilon_o m_i/n_o e^2)^{1/2}$$

whereas the equipartition time for electrons can be expected to scale as

$$\omega_{pe}^{-1} = (m_e/m_i)^{1/2}\omega_{pi}^{-1}$$

This argument is standard and should not predict unphysical results.

2. The ion thermal motion is negligible compared to the electrons ($T_e >> T_i$) so that ion dynamics are governed solely by the self-consistent electric field in the cold ion approximation to the equations of motion.

Thus we may write as the complete system of equations

$$\frac{\partial n}{\partial t} + \frac{\partial}{\partial x}(nu) = 0 \tag{2}$$

$$\frac{\partial u}{\partial t} + u\frac{\partial u}{\partial x} = \frac{\partial \psi}{\partial x} \tag{3}$$

$$\frac{\partial^2 \psi}{\partial x^2} = n - n_e(\psi) \tag{4}$$

where n and u represent the ion density and velocity scaled with respect to the undisturbed plasma density n_0 and the ion acoustic speed c. In addition, t is time measured in ion plasma periods ω_{pi}^{-1} and x is distance in electron Debye lengths λ_{De} with $\lambda_{De}\,\omega_{pi} = c$. Asymptotic conditions satisfied in the undisturbed plasma are given by

$$u,\ \psi,\ \frac{d\psi}{dx} \to 0\ ,\quad n \to 1 \quad \text{as } x \to \infty \tag{5}$$

The catalytic wall boundary condition links the dynamic behavior of the non-neutral sheath region with the continuing accumulation of charge on the wall. Using Gauss' law on a thin control volume surrounding the surface then gives

$$\frac{\partial E}{\partial t} = j_e(\psi_w) - nu \quad \text{at } x = 0 \tag{6}$$

and the boundary condition on ψ is then

$$\frac{d\psi}{dx} = E \quad \text{at } x = 0 \tag{7}$$

NUMERICAL RESULTS

We have integrated eqs. (2)-(4) numerically using a scheme similar to that of Widner et al. (ref. 12). First Poisson's equation is solved using a relaxation method with a variable convergence factor. The derivative boundary condition at x = 0 is incorporated into the relaxation using an image point technique and the asymptotic condition is satisfied by setting $\psi = 0$ at some x location sufficiently far into the plasma ($\psi = 0$ and x = 80 in the calculations presented here). The ion density and velocity are then advanced in time by numerically integrating the finite difference form of the continuity and momentum equations using the potential and electric field previously obtained. These updated n and u are then used to advance the electric field at the wall through eq. (6) which then serves to update the boundary condition (eq. 7) for the next iteration of Poisson's equation which now also includes an updated ion density. This procedure is then repeated until a steady state is reached. To start the calculation we assume the initial surface electric field to be caused by absorption of the random thermal electron flux through a matrix of stationary, uniform ions during an initial period of one electron plasma period. Poisson's equation was then solved with this initial field at $x = 0$ and the resulting potential and electron density distribution then served as "initial" conditions for the subsequent calculations. The distance and time spacings used were $\Delta x = .2$ and $\Delta t = .01$, with the x-axis divided into 400 intervals.

Figures (2 a) and (3 a) show plots of density and potential vs. x during the initial stage of charging for t = 0, 1, and 2. Figures (2 b) and (3 b) show the final stages of the approach to a steady state. The development of a non-neutral sheath region is clearly shown in these later times, with the sheath edge ($n \approx n_e$) moving into a quasineutral region of the plasma which has been pre-accelerated by an advancing ion acoustic disturbance. We note that neither the field nor potential vanishes at the sheath edge ($x_s \approx 15$ for $t = 72$) although the field is gradually diminishing in time. Furthermore, the wall potential ψ_w is within 3% of its floating value of 3.81 after only $10\ \omega_{pi}^{-1}$, although the electric field and ion flux at the wall take somewhat longer to approach their steady values of $E_w = -.716$ and $n_w u_w = -.382$, respectively.

In order to place the qualitative behavior of the sheath and plasma into better focus, consider the x-t diagram of fig. (4). The curve $x = \xi(t)$ represents the sheath edge, defined as the locus of points where $n \approx n_e$. Andrews (ref. 3) has shown that as long as $\dot{\xi}(t) > c$, no disturbance from the sheath and wall region may propagate into the undisturbed plasma. However, as the sheath edge decelerates through the point P_1 at which $\dot{\xi}(t_1) = c$, an ion acoustic rarefaction propagates into the plasma. As the sheath approaches the asymptotic steady state (shown for convenience at P_3), the constantly emitted rarefaction waves accelerate ions until at P_3 and beyond the sheath has reached a stable position, and the ions reach a steady final velocity entering the sheath, shown below to be the ion acoustic speed.

ANALYTICAL TREATMENT OF QUASINEUTRAL PLASMA

This composite picture of sheath development may be made quantitative by considering the equations of motion in the quasineutral region. Setting

$$n = n_e = e^{-\psi} \tag{8}$$

in eqs. (2) and (3) and neglecting Poisson's equation yields

$$\frac{\partial \ln n}{\partial t} + \frac{\partial u}{\partial x} + u \frac{\partial \ln n}{\partial x} = 0 \tag{9}$$

$$\frac{\partial u}{\partial t} + u\frac{\partial u}{\partial x} + \frac{\partial \ln n}{\partial x} = 0 \qquad (10)$$

The use of the equilibrium Boltzmann density for electrons (eq. 8) instead of the correct density as given by eq. (1a) is accurate to within about 1% for $t > 10$. The correct halfrange behavior should be retained only during the early stages of charging while the wall potential is still relatively small. Adding and subtracting these equations then gives the characteristic forms

$$\frac{D^{\pm}}{Dt} J^{\pm} = 0 \qquad (11)$$

where

$$J^{\pm} = u \pm \ln n \qquad (12)$$

$$\frac{D^{\pm}}{Dt} = \frac{\partial}{\partial t} + (u \pm 1)\frac{\partial}{\partial x} \qquad (13)$$

The solution to these equations is then

$$J^{\pm} = \text{const} \qquad (14)$$

on the characteristics $f^{\pm}$ defined by

$$\frac{dx}{dt} = u \pm 1 \qquad (15)$$

At this point several comments may be made about the resulting quasineutral plasma flow.

(i) The region beyond $\xi(t)$ is called a simple wave region since the $f^{\pm}$ characteristics are all straight lines. This may be seen by noting that at any point in the plasma

$$u = \frac{1}{2}(J^{+} + J^{-}) \qquad (16)$$

Now consider two adjacent points P' and P" on the characteristic f_2^{+} in fig. 4. It is clear from eq. (14) that $J^{+}(P') = J^{+}(P'')$. Furthermore, the quantity J^{-} is not only invariant along a given characteristic but, since all f^{-} characteristics originate in a region of constant state with $u = 0$ and $n = 1$, J^{-} is also the same on different f^{-} characteristics; therefore

$$J^{-}(P') = J^{-}(P'') = 0 \qquad (17)$$

where J^{-} has been evaluated in the undisturbed plasma. Consequently, $u' = u''$ and

$$\left.\frac{dx}{dt}\right|_{P'} = u' + 1 = u'' + 1 = \left.\frac{dx}{dt}\right|_{P''} \tag{18}$$

so that the slope of each f^+ characteristic is constant. Therefore, the f^+ characteristics represent lines of constant u and therefore also lines of constant $\ln n$.

(ii) It is clear that along the characteristic f_1^+

$$\left.\frac{dx}{dt}\right|_{1} = u_1 + 1 = 1 \tag{19}$$

since $u_1 = 0$. Furthermore, in order for the dynamical quantities to achieve steady values at the sheath edge, the asymptotic characteristic (shown for convenience as f_3) must be horizontal. Therefore,

$$\left.\frac{dx}{dt}\right|_{3} = u_3 + 1 = 0 \tag{20}$$

or

$$u_3 = -1 \tag{21}$$

Consequently, the rarefaction consists of a fan of straight line characteristics varying in slope from 1 to 0, which has the effect of accelerating the stationary ions to precisely the ion acoustic speed before appreciable charge separation may occur in the sheath.

Using eqs. (12), (14), (16), and (17) gives for point P'

$$u' = \frac{1}{2}(J^+ + J^-) = \frac{1}{2}[u_s + \ln n_s] \tag{22}$$

where u_s and n_s are the ion velocity and number at point P_2 on the sheath edge. Since u is constant on f_2^+

$$u' = u_s = \frac{1}{2}u_s + \frac{1}{2}\ln n_s \tag{23}$$

or

$$u_s = \ln n_s = -\psi_s \tag{24}$$

so that the f^+ characteristics are also lines of constant potential. Since $u_s < 0$, it is seen that $n_s < 1$ and $\psi_s > 0$.

This effectively solves the complete gas dynamic problem in the plasma region. However, to construct the solution explicitly requires knowledge of data along the sheath edge, which can only come in this self-consistent charging problem from using the relevant dynamical equations in the sheath itself obtained in the numerical solution.

We may, however, now completely describe the steady state sheath values and use these to check our numerical results. Using $u_s = -1$ as the steady ion velocity at the sheath edge then gives

$$u_s = -1\,, \quad \psi_s = 1\,, \quad n_s = e^{-1}$$

Now using the steady continuity and momentum equations for ions gives

$$n_w u_w = n_s u_s = -e^{-1}$$

$$u_w^{\,2} - 2\psi_w = u_s^{\,2} - 2\psi_s = -1$$

and the balance of ion and electron currents to the wall gives

$$-e^{-1} = n_w u_w = j_e(\psi_w) = -\left(\frac{m_i}{2\pi m_e}\right)^{1/2} e^{-\psi_w}$$

where we have again neglected the halfrange character of the electron distribution. The floating potential may then be found as

$$\psi_w = 1 + \frac{1}{2} \ln \frac{m_i}{2\pi m_e} = 3.84$$

and the ion velocity at $x = 0$ as

$$u_w = -\sqrt{2\psi_w - 1} = -2.60$$

An examination of the numerical solution then shows the floating potential (3.81) and the ion velocity at the wall (-2.61) are correctly computed to within 1% of the exact values found using the method of characteristics.

REFERENCES

1. Sander, K.F., J. Plasma Phys., 3, 353 (1969).
2. J.E. Allen and J.G. Andrews, J. Plasma Phys., 4, 187 (1970).
3. J.G. Andrews, J. Plasma Phys., 4, 603 (1970).
4. J.G. Andrews and R.H. Varey, Phys. Fluids, 14, 339 (1971).
5. C.H. Shih and E. Levi, AIAA Journal, 10, 104 (1972).
6. M.M. Widner and J.W. Poukey, Phys. Fluids, 19, 1838 (1976).
7. A.V. Gurevich, L.V. Pariĭskaya, and L.P. Pitaevskiĭ, Zh. Eksp. Teor. Fiz. 49, 647 (1965) [Sov. Phys. - JETP 22, 449 (1966)]; Zh. Eksp. Teor. Fiz. 63, 516 (1972) [Sov. Phys. - JETP 36, 274 (1973)].

8. J.E. Crow, P.L. Auer, and J.E. Allen, J. Plasma Phys., 14, 65 (1975).

9. M. Widner, I. Alexeff, and W.D. Jones, Phys. Fluids, 14, 795 (1971).

10. F.S. Felber and R. Decoste, Phys. Fluids, 21, 520 (1978).

11. P.N. Hu and S. Ziering, Phys. Fluids, 9, 2168 (1966).

12. M. Widner, I. Alexeff, W.D. Jones, and K.E. Lonngren, Phys. Fluids, 13, 2532 (1970).

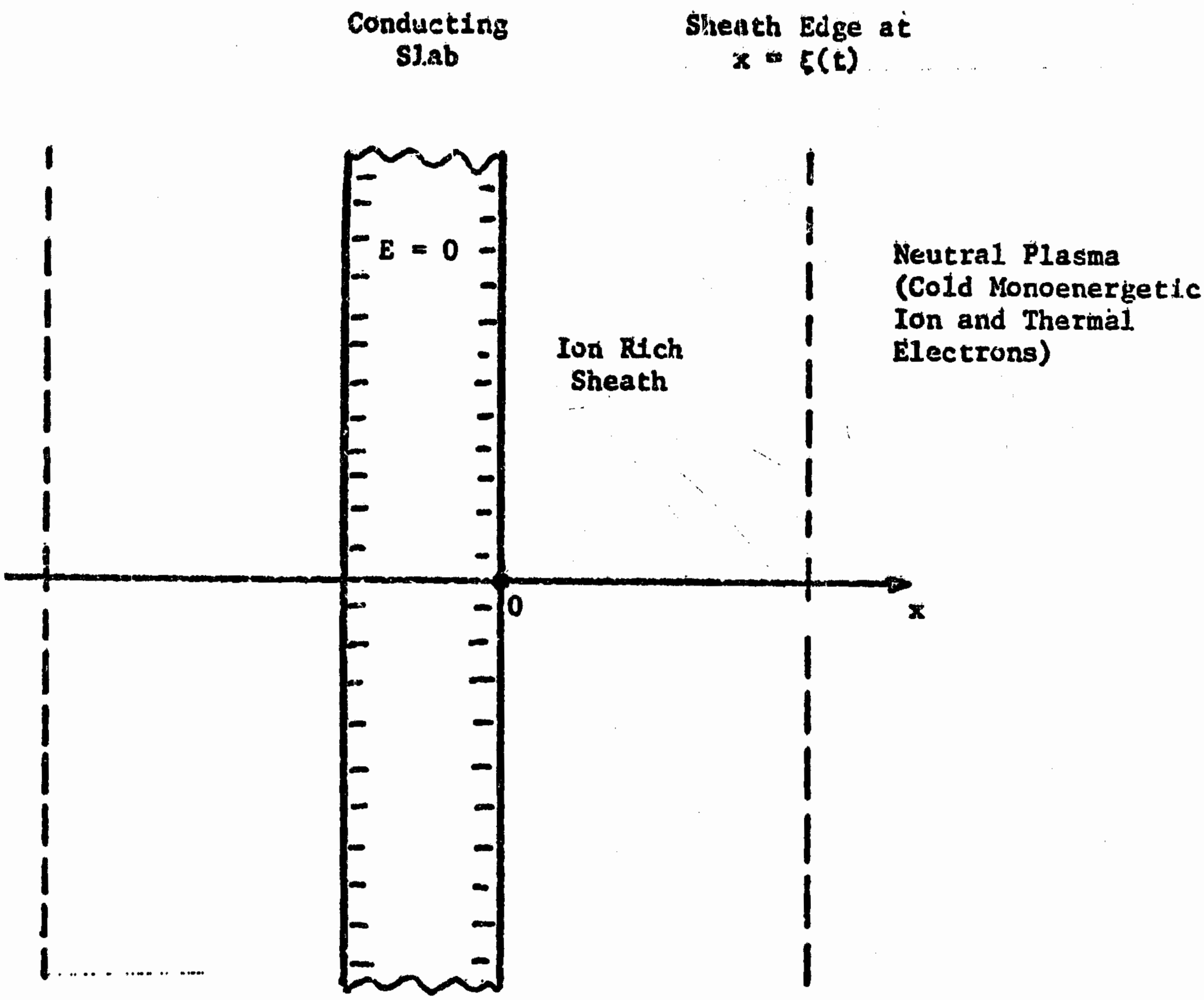

Figure 1. - Geometry.

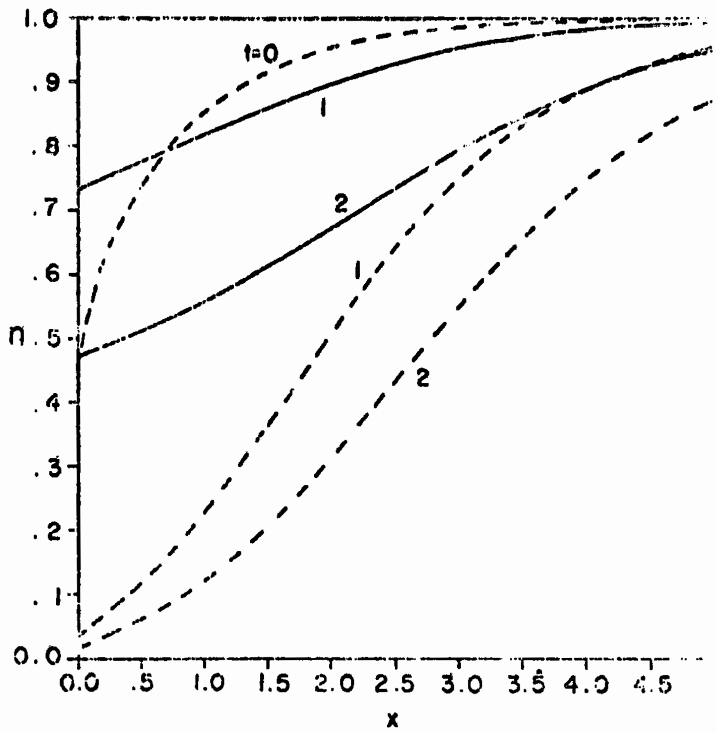

(a) Initial stage of charging.

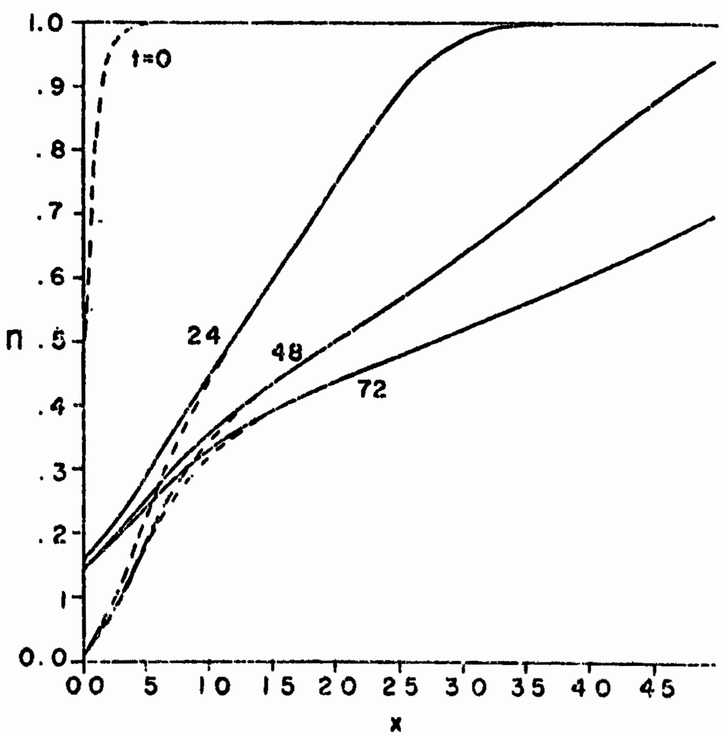

(b) Final stage of charging.

Figure 2. - Ion and electron densities as function of distance for several times in ω_{pi}^{-1} units. Electron densities are shown dotted.

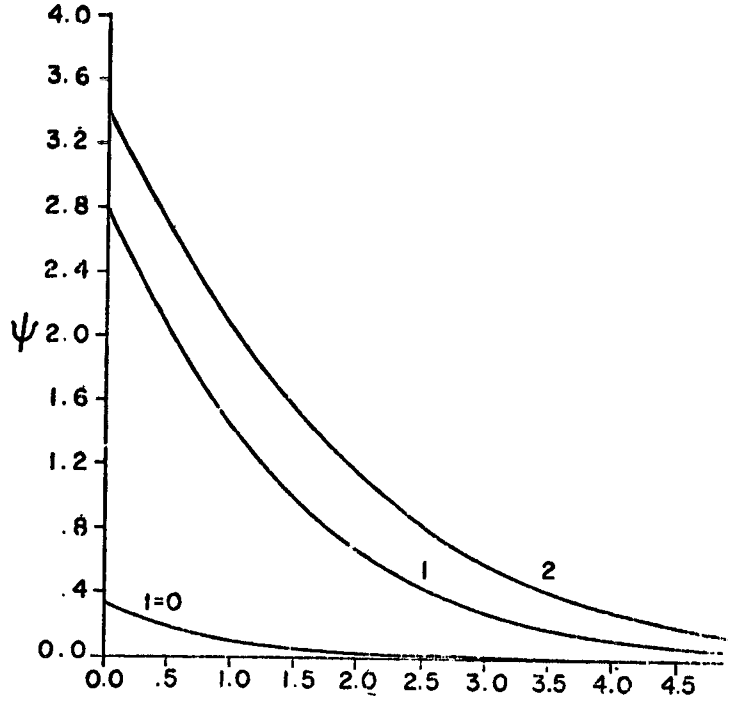

(a) Initial stage of charging.

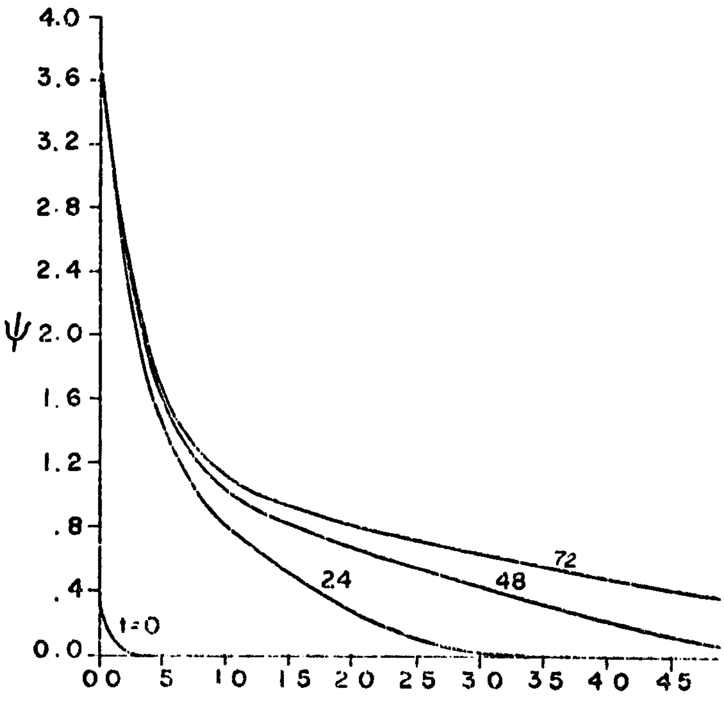

(b) Final stage of charging.

Figure 3. - Normalized potential as function of distance in Debye lengths for several times in ω_{pi}^{-1} units.

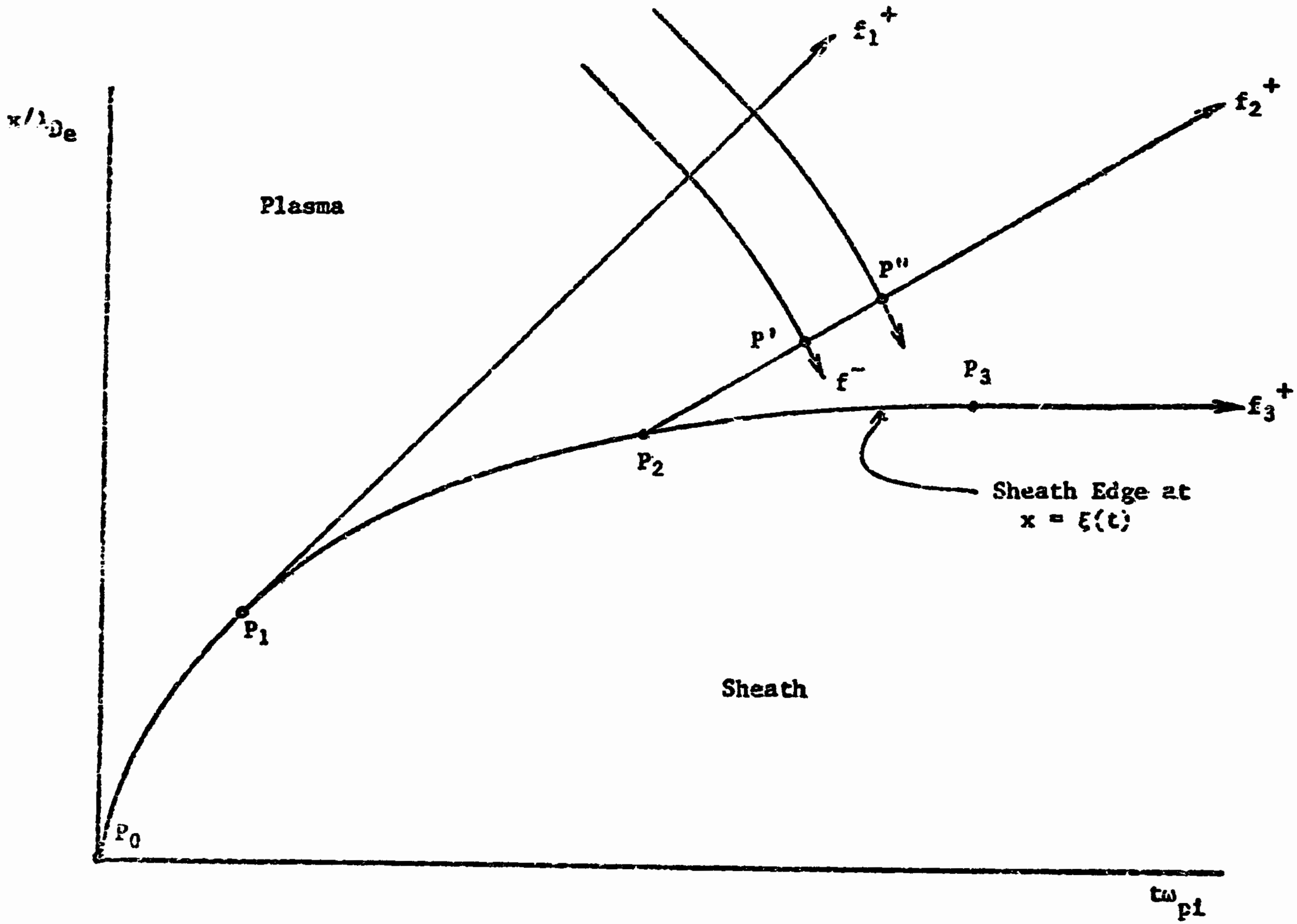

Figure 4 - Characteristic diagram for sheath edge motion.